

ANALYTICAL SEISMIC FRAGILITY CURVES FOR ANCIENT MASONRY BUILDINGS IN PORTUGAL

Vasco Bernardo ⁽¹⁾, Alfredo C. Costa ⁽²⁾, Paulo Candeias ⁽³⁾, Aníbal Costa ⁽⁴⁾, Paulo B. Lourenço ⁽⁵⁾

⁽¹⁾ Postdoctoral researcher, University of Minho (Department of Civil Engineering), vbernardo@civil.uminho.pt

⁽²⁾ Senior Researcher, National Laboratory for Civil Engineering (Structures Department), alf@lnec.pt

⁽³⁾ Invited Assistant Researcher, National Laboratory for Civil Engineering (Structures Department), pcandeias@lnec.pt

⁽⁴⁾ Full Professor, University of Aveiro (Department of Civil Engineering), agc@ua.pt

⁽⁵⁾ Full Professor, University of Minho (Department of Civil Engineering), pbl@civil.uminho.pt

Abstract

The seismic performance of buildings has received special attention due to the interest in the built heritage conservation and protection of human life. The historic urban centers are dominated by old unreinforced masonry (URM) buildings, which techniques and construction materials have evolved during centuries. Given the presence of these buildings in areas of significant seismicity, extensive research is needed to assess the seismic risk and define mitigation policies. This kind of studies is often supported by empirical methods and based on expert judgment due to the high variability of the building stock and lack of information. The main purpose of this work is to provide analytical fragility curves for representative masonry buildings in Portugal, built before the introduction of the first design code for building safety against earthquakes (RSSCS) in 1958. Thus, the fragility curves derived can characterize the capacity of the Portuguese building stock considering the randomness in the material properties and the variability in the geometry.

Keywords: pre-code masonry buildings; seismic probabilistic approach; seismic safety; seismic fragility analysis

1. Introduction

Over the years, masonry structures have shown evidence of good behavior under vertical static loads. However, its characteristics, such as the high specific mass, low tensile and shear strength, make the use of this heterogeneous material unsuitable in earthquake prone areas, e.g., Andradiva – Greece (2008), L'Aquila – Italy (2009), Emilia-Romagna – Italy (2012), Umbria – Italy (2016), Abruzzo – Italy (2017). Although Portugal has not been the target of high magnitude earthquakes in recent years, it remains susceptible, due to this geographical location, as it occurred in the past [1]: the 1755 Lisbon earthquake ($M_w = 8.5$), 1909 Benavente earthquake ($M_w = 6.3$), the 1969 Algarve earthquake ($M_w = 7.8$), Azores 1980 ($M_w = 7.2$) and 1998 ($M_w = 5.8$). These events caused significant damage in the affected regions, and particularly on masonry constructions [2].

The Portuguese building stock in historic urban centers is predominantly constituted by old unreinforced masonry (URM) residential buildings [3]. Their characteristics are the result of different periods of construction and construction practice due to the available materials, existing techniques, and society needs.

In the last decades, the performance of buildings under seismic action has received special attention due to the interest in the conservation of heritage and protection of human life. The seismic risk at a national scale was evaluated by [4] and [5], and by other authors at urban scale, e.g.: Coimbra [6], Faro [7], Seixal [8]. Most of these studies employed statistical data and expert opinion combined with empirical methods to derive fragility and vulnerability functions to characterize the building stock.

In order to support similar studies related to vulnerability and seismic risk assessment, this work aims to provide analytical fragility curves for the population of old (pre-code) URM buildings in Portugal with rigid and flexible floor diaphragms. Although the analyses carried out in the present work have been derived to account only for the in-plane mechanisms to be compliant with the current version of

EC8-3, which assumes these as being prevented from occurring, several works regarding out-of-plane fragility functions for masonry buildings can be found in literature, emphasizing the importance of such mechanisms, namely in buildings with flexible floor diaphragms [9]–[15].

In the framework of the present study, the development of the fragility curves involves the following steps: (i) generation of a synthetic database of 18.000 masonry buildings up to 5 stories high, including different archetypes based on statistical information previously collected and different material properties to cover the variability found in the literature; (ii) estimate the in-plane seismic behavior of the entire database through displacement-based nonlinear static methods; (iii) derivation of fragility functions for the capacity expressed by the maximum interstorey drift. The fragility curves proposed are only related to the deformation capacity of the buildings in order to be applied in seismic risk studies or safety assessment.

2. Old masonry buildings description

Four typologies of masonry buildings are typically identified in the urban centers of Portugal (Figure 1.): “Pre-Pombalino” (before 1755), “Pombalino” (1755 to 1870), “Gaioleiro” (1870 to 1930) and “Placa” (1930 to 1960). The “Pre Pombalino” buildings, constructed before the 1755 earthquake, are recognized by their irregular geometry, reduced dimensions, narrow facades, high density of walls and few openings to the exterior. They usually are four stories high and are constituted by poor-quality masonry walls supporting the timber floors. The “Pombalino” buildings emerged after the Lisbon earthquake and are particularly known by the improvements in the anti-seismic conception in that period. They usually have up to five stories high and regular geometry. This typology was standard in the building construction practice for more than one century. On the other hand, the “Gaioleiro” buildings represent a downgrade when compared to the previous typology, with the adoption of more simplified construction techniques and the use of low-quality materials which was promoted by the rapid expansion of the urban centers and the housing demand. This typology is significantly more vulnerable, from a seismic point of view, compared with the previous one. Finally, “Placa” buildings emerged before the enforcement of the first seismic-code in 1958 and introduced the use of lightly reinforced concrete slabs at the floors level. The high mass of the RC slabs and the low strength capacity of the load bearing walls to horizontal forces results in an unsatisfactory structural seismic performance. The main characteristics of these typologies are briefly described in Figure 1.



Figure 1 Main features of old masonry buildings

3. Geometry of representative masonry buildings

3.1 Geometry characterization and definition of archetypes

The geometry characterization comprises the information gathered through detailed drawings from the original projects and collected from municipal archives, for a population of 100 old (pre-code) masonry buildings. This data represents the geometry for the most typical masonry buildings built before the decade of 1960 and described in the previous section. The geometric parameters obtained, such as plan dimensions, height of the stories, openings ratio, interior walls density, walls thickness and type/thickness of floors, were statistically characterized and described in Bernardo *et al.* 2021.

Based on this information, 9 archetypes – A1, A2, A3, B1, B2, B3, C1, C2 and C3 – with different configurations and up to 5 stories high, were generated for the subsequent analyses. Figure. 2 presents the layout of these archetypes. Table 1 summarizes the statistical information for the geometry and the parameters adopted (underlined) to represent the archetypes.

The archetype B2 (Figure. 2) represents the mean size configuration (12.6x12.1m). The plan dimensions for the remaining were derived from the mean archetype, considering a dispersion equals to one standard deviation: $L_x = 12.6 \pm 5.0\text{m}$ and $L_y = 12.1 \pm 4.1\text{m}$. The total area ranges approximately between 60.0m^2 to 285.0m^2 . The layout for the arrangement of the partitions/interior walls follows, in a reasonable manner, the typical size of the compartments for these typologies (3x3m up to 4x5m), representing a mean value for the interior walls' density equal to 0.054.

Regarding the walls thickness, considering the enormous variability in the type of material, arrangement and absence of information in the documentation gathered, were considered the mean thickness for the facades and side walls. For the interior/partition walls the most common value (mode) were adopted, which are representative for more than 60% of the buildings collected [20]. The intrinsic variability in the wall's characteristics (type of masonry, morphology and arrangement) was computed in the material mechanical properties uncertainty, carried out in section 3.2. For the remaining variables, the mean values adopted are mentioned in Table 1.

Table 1 Statistical properties for the geometric parameters [20]

Statistical properties	L_x [m]	L_y [m]	IWD [-]	H_0 [m]	H_n [m]	OR _F [-]	OR _B [-]	Th ₁ [m]	Th ₂ [m]	Th ₃ [m]	Th ₄ [m]	AWTR [-]
Mean μ	<u>12.6</u>	<u>12.1</u>	<u>0.054</u>	<u>3.23</u>	<u>3.01</u>	<u>0.23</u>	<u>0.21</u>	<u>0.47</u>	<u>0.34</u>	0.21	0.14	<u>0.11</u>
Std. deviation σ	<u>5.00</u>	<u>4.1</u>	0.01	0.42	0.24	0.08	0.08	0.14	0.11	0.05	0.02	0.06
mode	-	-	-	-	-	-	-	-	-	<u>0.25</u>	<u>0.15</u>	0.10

L_x and L_y – size; H_0 and H_n – ground and upper floor stories high; OR – openings ratio: front (OR_F) and back (OR_B) facade; IWD – interior walls density; Th – walls thickness: facades (1), lateral side (2), interior (3), partition (4); AWR – average walls thickness reduction on the facade

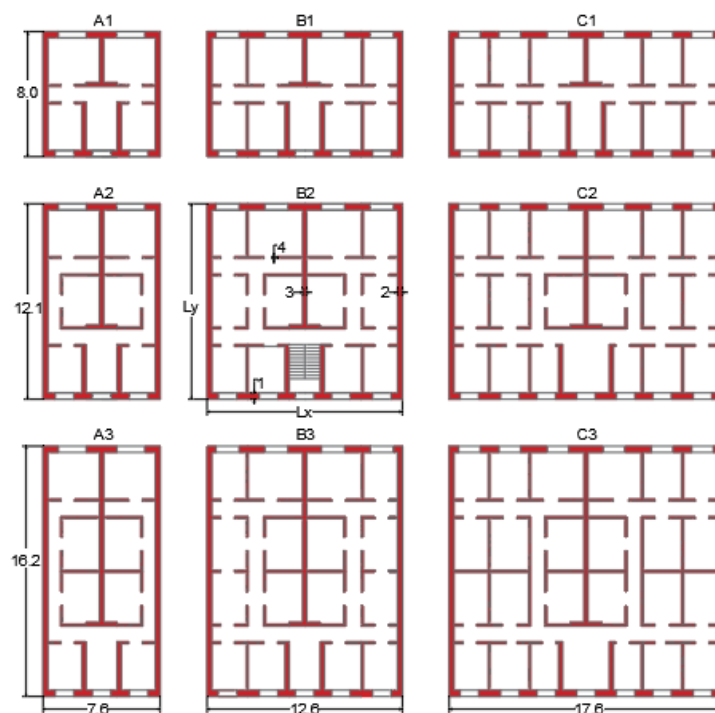


Figure. 2 Archetypes adopted to represent the population of old masonry buildings in Portugal

3.2 Material properties selection

The definition of material mechanical properties was based on literature review, which includes the masonry properties that can be identified in the Portuguese building stock and the suggested properties by the latest version of EC8-3 (see Candeias *et al.* 2020).

Taking into account the wide range of masonry mechanical properties, the uncertainty was propagated through *Monte Carlo* simulations [22]. For that purpose, two groups of buildings were considered with different material properties (see Table 2): *Type I* – typologies with good quality masonry (e.g., regular and squared masonry, brick masonry with cement lime mortar) and *Type II* – typologies with poor quality masonry (e.g., rubble stone masonry, brick masonry with lime mortar). Given the differences of the interior/partition walls (e.g., *tabique*¹, *frontal walls*², perforated brick masonry) when compared with the exterior walls (e.g., solid masonry bricks, stone masonry or concrete blocks), two sub categories were defined: *Type I-1* and *Type II-1*, to represent the properties of exterior walls, and *Type I-2* and *Type II-2* for the interior/partition walls. A set of 100 samples for each typology – Type I and Type II – were generated to describe the material variability, attaining an error of around 5% (95% confidence interval) for the material population generated.

Table 2 Mean values and dispersion adopted for the material mechanical properties

Random variable	Distribution	COV	Mean value			
			Type I-1	Type I-2	Type II-1	Type II-2
Compressive strength f_c [MPa]	LogNormal	0.40	5.00	2.00	2.50	1.25
Factor K * [-]	Truncated Normal	0.25	800 (250 - 1100)			
Young's modulus E [MPa]	-	-	4000	1600	2000	1000
Shear modulus G [MPa]	LogNormal	0.40	1700	650	850	450
Density ρ [kg/m ³]	Normal	0.10	1800	1200	1800	1200
Cohesion τ_0 [MPa]	LogNormal	0.40	0.15	0.15	0.07	0.07
Friction coefficient μ^{**} [-]	LogNormal	0.40	0.40	0.40	0.40	0.40

* Factor k correlates the Young's modulus and compressive strength: $E = K \cdot f_c$
** According to EC8-3

4. Numerical modelling assumptions

4.1 Modelling strategy and general assumptions

Considering the previous geometric statistical information, tridimensional multi degree of freedom models (MDOF) were developed to simulate the nonlinear response of the buildings. For this purpose, an equivalent frame modeling strategy available in the research version (2.1.104) of *TREMURI* software [23] was used. Some of the features of the model include the accurate representation of the principal in-plane failure mechanism, including the stiffness and strength degradation, such as bending rocking, diagonal shear and sliding.

The software was originally developed for frame-type analysis of the entire URM buildings whereby the response is governed by the in-plane behavior of the walls. On the other hand, the current version of EC8-3 also does not include the out-of-plane mechanisms or assumes these as being prevented from occurring. Hence, the behavior of the buildings analyzed is only restricted to in-plane mechanisms.

4.2 Macroelement model validation

The macroelement model is defined by a set of mechanical parameters at macroscopic scale that should be representative of an average of the masonry panel properties: Young's modulus – E , shear modulus

¹ set of vertical long boards connected by horizontal small wood stripes, normally filled with pieces of bricks and lime mortar

² set of plane wood trusses very common in "Pombalino" typology

– G , density – ρ , compressive strength – f_c , cohesion – τ_0 , friction coefficient – μ , and by two phenomenological parameters related to the shape of nonlinear shear constitutive model – c_t that expresses the shear deformability in the inelastic range, wherein the amplitude in the inelastic displacement is proportional to the product Gc_t ; and β_s that controls the slope of the softening branch in the post-peak region [23].

The validation of the macroelement model was performed using the results of an in-plane quasistatic experimental test carried out on a full-scale masonry panel, with aspect ratio of 1.325:1 (2.65x2.00x0.25m – height, length and thickness), made of solid clay bricks, extracted from an old masonry building. Further details can be found in [24].

4.3 Floor diaphragms modelling

Floor diaphragms were modelled as a two-dimensional orthotropic membrane element, defined by four nodes with two displacement degrees of freedom each, and characterized by the equivalent mechanical properties: equivalent thickness – t_{eq} , modulus of elasticity of the diaphragm in the principal direction – E_1 – and perpendicular direction – E_2 , shear modulus – G , that influence the horizontal force distribution between walls, and Poisson ratio – ν .

Two types of floor diaphragms, rigid and flexible, were considered. Rigid diaphragms were modelled by RC slabs and assuming a load distribution in the walls proportional to the influence area. In this case, it was assumed a good connection between the walls to ensure equal planar displacements at floor level, simulated through rigid links beams. A typical timber floor was adopted for flexible diaphragms, constituted by timber sheathing and timber joists perpendicular to the facades. In this case, the load was distributed by the main timber joists and the connections between walls were modelled through equivalent elastic link beams at the floor level to simulate medium to weak connections, according to [25]. Table 3 and Table 4 summarize the mechanical properties for the membrane elements (rigid and flexible) and for the connection between walls, respectively.

Table 3 Mechanical properties adopted for the floor diaphragms

Type of floor	Equivalent thickness t_{eq} [m]	Elastic modulus E_1 [GPa]	Elastic modulus E_2 [GPa]	Shear Modulus G [GPa]	Poisson coefficient ν [-]
Rigid	0.20	30.0	30.0	13.0	0.20
Flexible [25]	0.022	29.0	12.0	0.011	-

Table 4 Parameters adopted to simulate the connections between walls [25]

Type of connections	Area A [m ²]	Inertia I [m ⁴]	Elastic modulus E [GPa]
Good (rigid)	10.0	5.0	30.0
Medium to weak (flexible)	0.0004	0.0002	

4.4 Representative buildings models

Considering the assumptions related to geometry layout and discussed in previous sections, 45 archetypes of buildings were modelled (A1, A2, A3, B1, B2, B3, C1, C2 and C3), up to 5 stories high, as shown in Figure. 3. Attending to materials variability and different type of floor diaphragms (rigid and flexible), a population of 18000 buildings was generated, based on the modelling assumptions previously described. With regard to gravity loads applied, the prescriptions of Eurocode 8 [26] are followed, combining the nominal values of permanent loads G with the quasi-permanent live loading $\Psi_E Q$. The permanent loads are defined by the self-weight of the masonry, timber floors (1.10 kN/m²) and timber roof (1.30 kN/m²). The live loads depend on the building category, which is assumed for domestic and residential purpose (category A).

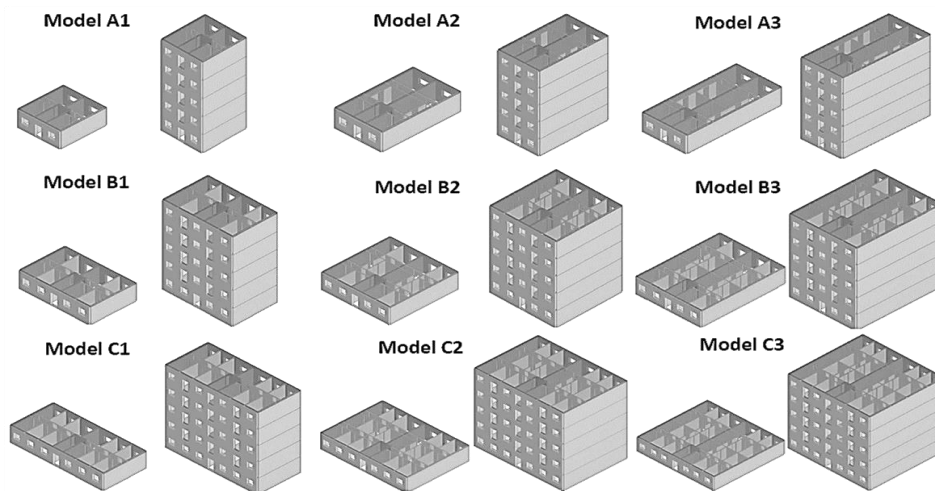


Figure. 3 Archetypes of masonry old buildings modelled in TREMURI

5. Numerical analysis and seismic behavior

5.1 Methodology for seismic assessment

In order to develop the fragility curves compatible with the current version of EC8-3, the methodology to evaluate the seismic behavior of the buildings follow the recommendations of the standards for the in-plane global safety verification using nonlinear methods.

The general methodology of EC8-3 uses a performance- and displacement-based approach to assess the safety level of a given structure. Regarding the required performance levels for Portugal, implicitly related to the seismic hazard, three limit states (LS) are defined to assess the structural performance of an existing building, depending on its importance class: Damage Limitation (DL), Significant Damage (SD) and Near Collapse (NC). The return periods (RP) prescribed by EC8-3 for these LS are defined in accordance with levels of protection, having values of 73, 308 and 975 years for the DL, SD and NC limit states, respectively, corresponding to probabilities of exceedance of 50%, 15% and 5% in 50 years. For residential buildings (importance class II) the safety verification is only mandatory for the SD limit state.

5.2 Nonlinear static analysis

The buildings' capacity was predicted from nonlinear numerical static analysis (pushover), through monotonic horizontal forces, which requires particular attention on the choice of load pattern. In general, design codes propose to assume two load patterns (e.g., uniform and triangular) to simulate the distribution of inertial forces during the seismic loading on the deformed shape of the buildings. However, the deformed shape depends on the damage on the building and may change during the loading scenario. To overcome this limitation, [29] propose an adaptive pushover algorithm for masonry buildings, wherein the load pattern is proportional to the displacement shape in the previous step. This approach revealed to be more suitable for masonry buildings with rigid floors, comparing with time-history analysis. However, for flexible floors, given the local mechanisms and the mass participation of each single wall in the vibration mode, that approach does not provide significant improvements. In that case, the pseudo-triangular load pattern is better suited to assure that all mass is mobilized [30]. For the present study, adaptive pushover analyses with inverse triangular first ratio pattern were adopted for buildings with rigid floors and an inverted pseudo-triangular for flexible floors. The control node was selected at the top level and the shear was measured on the base up to reaching 20% decay of the maximum shear strength (NC limit state), as recommend by the EC8-3 for a global safety verification. Figure. 4 presents the capacity curves normalized for spectral acceleration S_a and spectral displacement S_d for the archetypes A1, B2, and C3, with 3 to 5 stories high. The red and blue dots correspond to the

maximum shear strength and the ultimate displacement for the NC limit state, respectively. The results are presented for the seismic action in the longitudinal direction (parallel to the facade walls), which revealed to be more critical for the geometry layout defined by exterior lateral walls without openings.

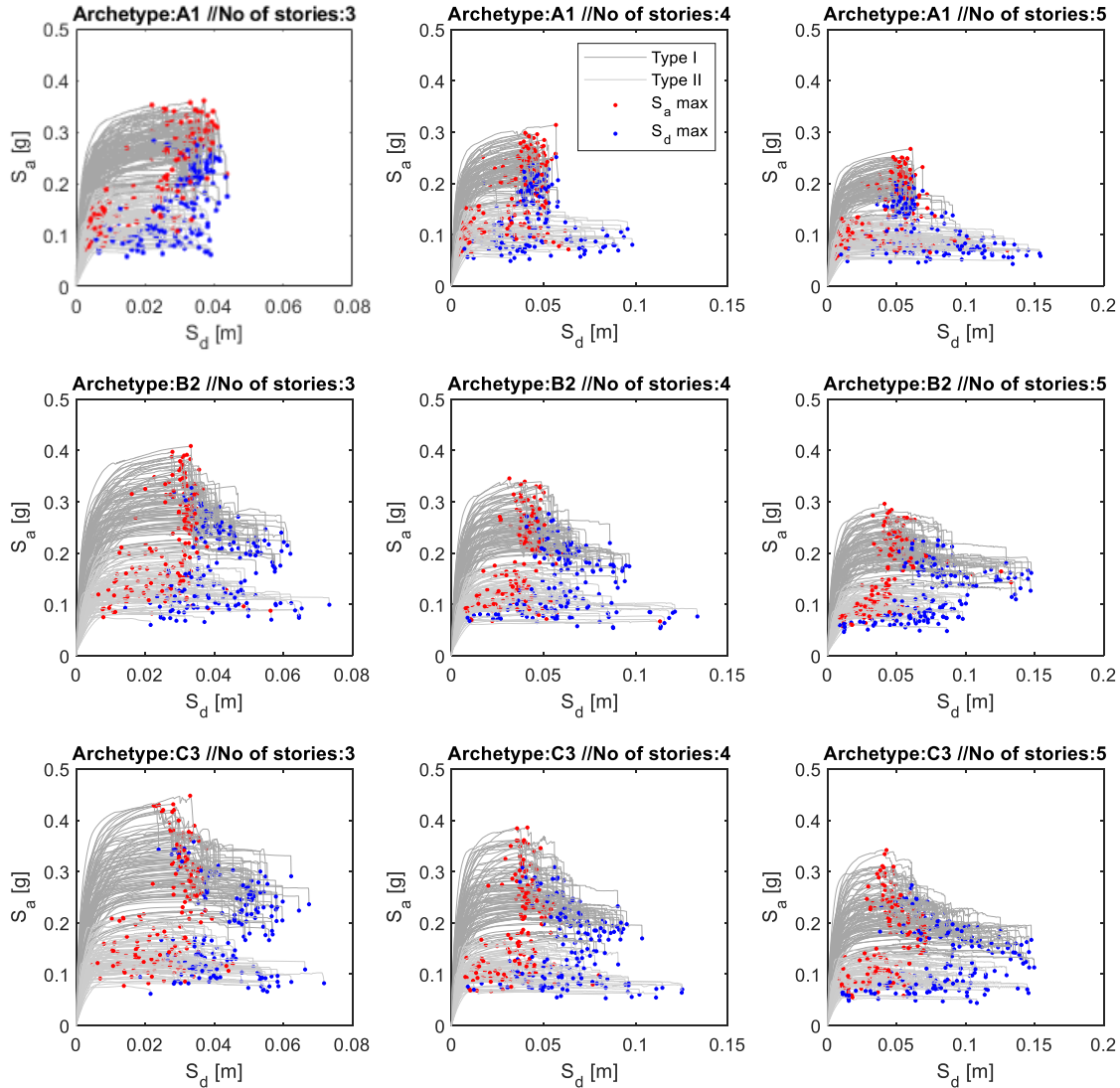


Figure. 4 Capacity curves for archetypes A1, B2 and C3, with 3, 4 and 5 stories height and rigid floors

5.3 Seismic performance-based assessment

In this study, the seismic performance was evaluated for each building, adopting the response spectrum for the seismic action offshore (seismic action type 1) and inland (seismic action type 2) defined in EC8-1 for Portugal, an equivalent viscous damping equal to 5%, soil amplification factor corresponding to a soil type A, B and C, and a wide range of return periods (RP) up to 5000 years. Taking the 475-years RP as the reference period RP_{ref} , the acceleration on the ground a_g can be scaled to other RP as suggested in the comments to the Portuguese version of EC8-1: $a_g = a_{gr}(RP_{ref}/RP)^{-1/k}$, where a_{gr} is the acceleration for the RP_{ref} and k take the values of 1.5 and 2.5 for seismic action in mainland offshore and onshore, respectively, and 3.6 for Azores. These coefficients assume the mean values obtained in the counties and a first-order power law approximation for the seismic hazard.

6. Seismic fragility analysis

In the present work, the limit state (LS) thresholds follow the global scale criterion as a percentage of maximum shear (F_{max}) defined in the capacity curves, which are in line with the LS proposed by the EC8-3. Therefore, the LS are expressed in terms of spectral displacement (S_d) as a function of the base shear measured, according to criteria indicated in Table 5. The LS1 was defined at the yielding point of the idealized capacity curve and LS2 and LS3 correspond to the peak of maximum shear and post-peak range, respectively.

Table 5 Damage state definition for unreinforced masonry buildings

Limit state	Performance Level	Description	Criteria
LS1 – DL	Immediate Occupancy: Damage Limitation	Minor structural damage; moderate non-structural damage	S_{dy}
LS2 – SD	Life Safety: Significant Damage	Significant structural damage; extensive non-structural damage.	$S_d (F_{max})$
LS3 – NC	Collapse Prevention: Near Collapse	Near collapse; repairing the building is not feasible	$S_d (0.80F_{max})$

The fragility curves proposed in this section were derived from empirical cumulative distribution functions (CDF) for the data analyzed, directly obtained from the nonlinear response of the buildings, considering the limit states indicated in Table 5. Therefore, the fragility curves presented are independent of the seismic action, or spectrum format, and represent the capacity exceedance probability conditioned on a value of demand for the three limit states adopted.

For this purpose, the archetypes were grouped and analyzed by number of stories, typology (Type I and Type II) and type of floor diaphragm rigid (RD) or flexible (FD). The best cumulative analytical function was fitted to the data based on Kolmogorov-Smirnov tests, and follow, in a reasonable manner, a LogNormal (LN) and Weibull (W) distribution for typologies Type I and Type II, respectively. Figure 6 presents the proposed fragility curves, expressed as a function of interstorey drift θ_C , by number of floors, typology and type of floor diaphragm. Table 6 summarizes the median values of θ_C and dispersion β_D for the analytical fragility functions proposed for the buildings' capacity. Note that, the values of dispersion achieved in this section include the randomness in material properties defined for each typology and the variability in the geometry layout of the archetypes, allowing to account both variables in the capacity of the buildings for seismic risk studies or seismic assessment.

Bar chart of Figure 5 presents a comparison of the moments proposed for the different typologies, type of floor diaphragm and number of stories, to support the discussion of results. For the mean values θ_C (%) computed, the main differences are observed between typologies and type of floor diaphragm: Type I/RD 0.09 to 0.12 (DL), 0.37 to 0.47 (SD), 0.45 to 0.70 (NC); Type II/RD 0.07 to 0.09 (DL), 0.22 to 0.31 (SD), 0.38 to 0.70 (NC); Type I/FD 0.21 to 0.40 (DL), 0.65 to 0.91 (SD), 0.70 to 1.09 (NC); Type II/FD 0.23 to 0.33 (DL), 0.51 to 0.75 (SD), 0.70 to 0.91 (NC). As can be noticed, high values of θ_C are attained for structures with FD and mostly for type I typology. In contrast, the type II-rigid presents minor drifts, followed by the type I-rigid. In general, buildings with good quality masonry (Type I) present higher values of θ_C , except for one storey height with FD.

Regarding the dispersion β_D , the range of values vary from: Type I/RD \rightarrow 0.30 to 0.33 (DL), 0.12 to 0.26 (SD), 0.15 to 0.32 (NC); Type II/RD \rightarrow 0.41 to 0.51 (DL), 0.50 to 0.58 (SD), 0.20 to 0.50 (NC); Type I/FD \rightarrow 0.20 to 0.40 (DL), 0.19 to 0.30 (SD), 0.22 to 0.33 (NC); Type II/FD \rightarrow 0.27 to 0.62 (DL), 0.34 to 0.60 (SD), 0.30 to 0.50 (NC). Thus, in general, the values of dispersion attained are higher for typology Type II. For the same typology, minor differences between the number of floors are noticed, except for buildings with one story. For the SD limit state, the dispersion has a slight range between the number of floors, comparing to the other limit states, excluding the Type II-flexible typology with relatively similar dispersion. Finally, for the DL seems to be some trend for lower dispersion in low-rise buildings, in contrast to the higher dispersion computed in taller buildings for the NC limit state.

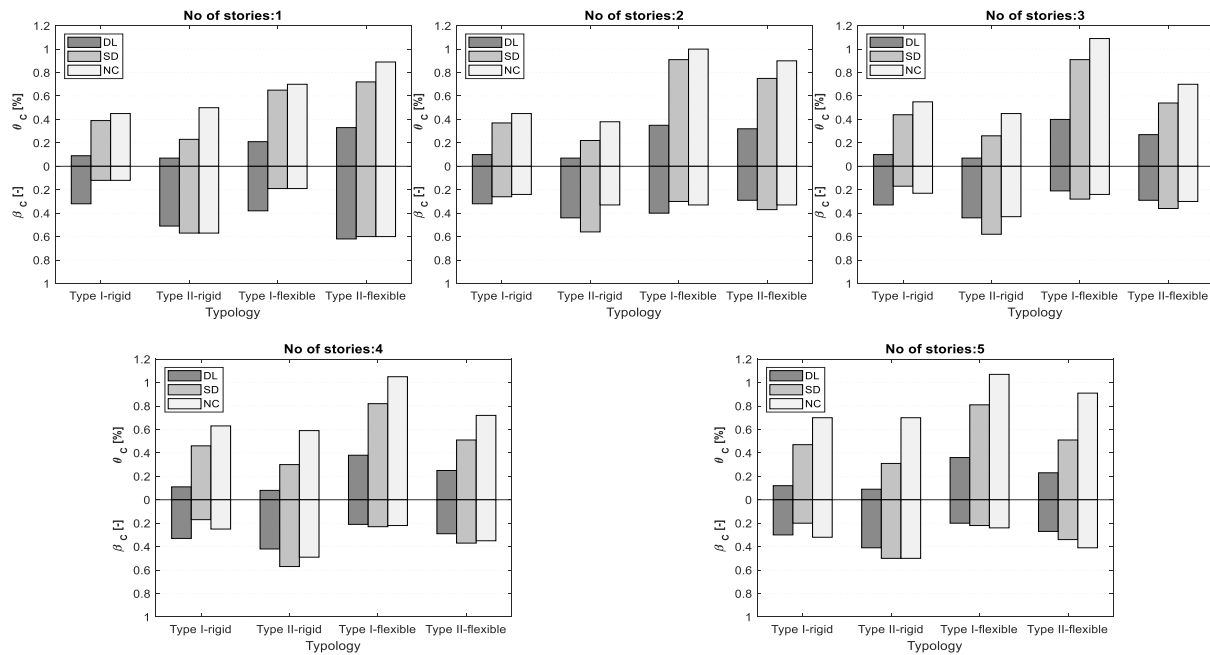


Figure. 5 Analytical fragility curves proposed for the buildings' capacity: comparison of the median θ_c and dispersion β_c values by number of stories, typology and type of floor diaphragm.

Table 6 Moments of the analytical fragility curves proposed for the buildings' capacity.

No of stories	Typology	Function	LS1 – DL				LS2 – SD				LS3 – NC			
			θ_c	β_c	a	b	θ_c	β_c	a	b	θ_c	β_c	a	b
1	Rigid-Type I	LogN	0.09	0.32	-	-	0.39	0.12	-	-	0.45	0.15	-	-
	Rigid-Type II	Weibull	0.07	0.51	0.08	2.05	0.23	0.57	0.26	1.83	0.50	0.20	0.54	5.80
	Flexible-Type	LogN	0.21	0.38	-	-	0.65	0.19	-	-	0.70	0.22	-	-
	Flexible-Type	Weibull	0.33	0.62	0.43	1.75	0.72	0.60	0.87	2.63	0.89	0.50	1.04	2.91
2	Rigid-Type I	LogN	0.10	0.32	-	-	0.37	0.26	-	-	0.45	0.24	-	-
	Rigid-Type II	Weibull	0.07	0.44	0.07	2.41	0.22	0.56	0.25	1.85	0.38	0.33	0.42	3.33
	Flexible-Type	LogN	0.35	0.40	-	-	0.91	0.30	-	-	1.00	0.33	-	-
	Flexible-Type	Weibull	0.32	0.29	0.36	3.92	0.75	0.37	0.82	3.07	0.90	0.33	1.03	3.60
3	Rigid-Type I	LogN	0.10	0.33	-	-	0.44	0.17	-	-	0.55	0.23	-	-
	Rigid-Type II	Weibull	0.07	0.44	0.08	2.42	0.26	0.58	0.29	1.79	0.45	0.43	0.50	2.47
	Flexible-Type	LogN	0.40	0.21	-	-	0.91	0.28	-	-	1.09	0.24	-	-
	Flexible-Type	Weibull	0.27	0.29	0.30	3.84	0.54	0.36	0.59	2.79	0.70	0.30	0.80	3.80
4	Rigid-Type I	LogN	0.11	0.33	-	-	0.46	0.17	-	-	0.63	0.25	-	-
	Rigid-Type II	Weibull	0.08	0.42	0.09	2.56	0.30	0.57	0.34	1.83	0.59	0.49	0.67	2.17
	Flexible-Type	LogN	0.38	0.21	-	-	0.82	0.23	-	-	1.05	0.22	-	-
	Flexible-Type	Weibull	0.25	0.29	0.27	3.84	0.51	0.37	0.55	2.71	0.72	0.35	0.82	3.36
5	Rigid-Type I	LogN	0.12	0.30	-	-	0.47	0.20	-	-	0.70	0.32	-	-
	Rigid-Type II	Weibull	0.09	0.41	0.10	2.61	0.31	0.50	0.34	2.09	0.70	0.50	0.79	2.12
	Flexible-Type	LogN	0.36	0.20	-	-	0.81	0.22	-	-	1.07	0.24	-	-
	Flexible-Type	Weibull	0.23	0.27	0.25	4.28	0.51	0.34	0.53	3.55	0.91	0.41	0.90	2.84

a, b are, respectively, the scale and shape parameter for the Weibull distribution

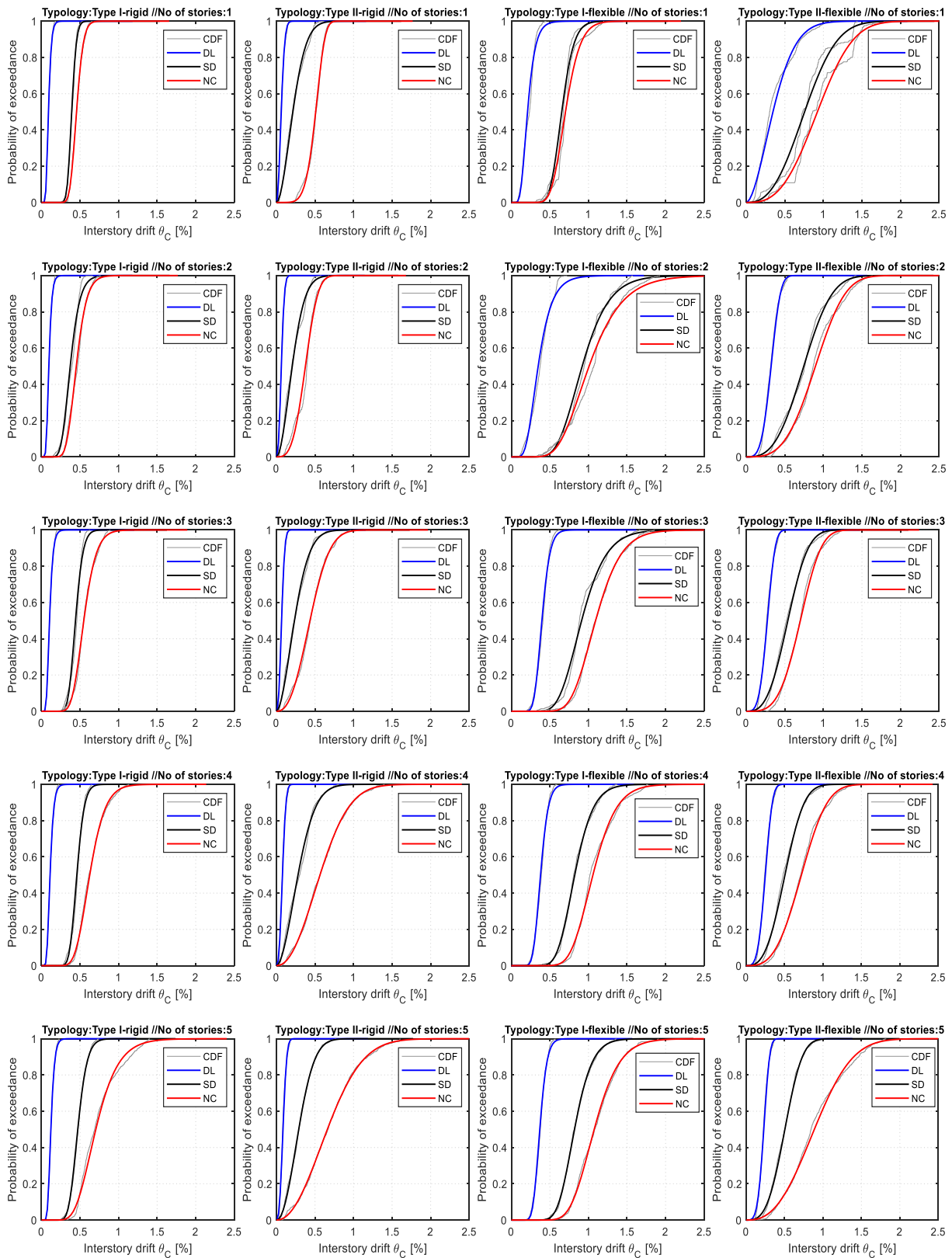


Figure. 6 Analytical fragility proposed curves for the buildings' capacity expressed by θ_C .

7. Final comments and conclusions

Seismic risk studies are of extreme importance in regions with moderate to high seismicity, such as Portugal, to estimate losses and establish policies for risk mitigation. This kind of studies requires knowledge about the building stock, which is often characterized by empirical methods and expert opinion when performed at large scale. The main purpose of the present paper was to derive analytical fragility curves that can be used to conduct more detailed seismic risk studies or employed for seismic assessment of pre-code masonry buildings.

The development of the proposed fragility curves considered a synthetic database of 18.000 masonry buildings, based on statistical information previously collected about the geometry, allowing to define nine archetypes (A1, A2, A3, B1, B2, B3, C1, C2, C3), which were further combined with a wide range of material properties (Type I – good quality and Type II – poor quality) and type of floor diaphragm (rigid and flexible).

Based on the previous analyses, analytical fragility curves for the buildings' capacity were derived for both typologies and type of floor diaphragm. Among the results gathered, the following stand out: i) buildings with good quality materials and flexible diaphragm (Type I FD) reach higher drift values (up to 0.41% DL, 0.91% SD and 1.09% NC). In contrast, smaller drifts (up to 0.09% DL, 0.31% SD and 0.70% NC) are attained for structures with poor quality masonry and rigid diaphragm (Type II RD); ii) the dispersion achieved is higher in Type II FD buildings (up to 0.62 DL, 0.60 SD and 0.50 NC) and smaller in Type I RD buildings (up to 0.33 DL, 0.26 SD and 0.32 NC); iii) in general, drift values and respective dispersion seems to be higher with the increase in number of floors.

The proposed fragility curves are not linked to a ground motion intensity, or spectrum format, and can be applied in a more general context to characterize the capacity of the building stock considering the randomness in the material properties and the variability in the geometry.

Acknowledgements

Foundation for Science and Technology (FCT) under Grant number PD/BD/135325/2017 in the scope of the InfraRisk Doctoral Programme. STAND4HERITAGE project that has received funding from the European Research Council (ERC) under the European Union's Horizon 2020 research and innovation program (Grant agreement No. 833123), as an Advanced Grant.

References

- [1] C. S. Oliveira, "A sismicidade historica e a revisao do catalogo sismico. National Laboratory for Civil Engineering. Report 36/11/7368." National Laboratory for Civil Engineering, Lisbon, Portugal [in Portuguese], 1986.
- [2] M. R. Correia, P. B. Lourenço, and H. Varum, *Seismic retrofitting: Learning from vernacular architecture*. Taylor & Francis. 1st edition. ISBN 9781138028920. 2015.
- [3] INE, "Censos 2011 Resultados Definitivos. Report," Lisbon, Portugal [in Portuguese], 2012.
- [4] M. L. Sousa, "Seismic risk in Mainland Portugal," Technical University of Lisbon, Lisbon, Portugal [in Portuguese], 2006.
- [5] V. Silva, H. Crowley, H. Varum, and R. Pinho, "Seismic risk assessment for mainland Portugal," *Bulletin of Earthquake Engineering*, 2014.
- [6] R. Vicente, S. Parodi, S. Lagomarsino, H. Varum, and J. Silva, "Seismic vulnerability and risk assessment: Case study of the historic city centre of Coimbra, Portugal," *Bulletin of Earthquake Engineering*, 2011.
- [7] R. Vicente, T. Ferreira, and R. Maio, "Seismic Risk at the Urban Scale: Assessment, Mapping and Planning," *Procedia Economics and Finance*, 2014.
- [8] T. M. Ferreira, R. Vicente, J. A. R. Mendes da Silva, H. Varum, and A. Costa, "Seismic vulnerability assessment of historical urban centres: Case study of the old city centre in Seixal, Portugal," *Bulletin of Earthquake Engineering*, vol. 11, no. 5, pp. 1753–1773, Oct. 2013.
- [9] G. Sumerente, H. Lovon, N. Tarque, and C. Chácará, "Assessment of combined in-plane and out-of-plane fragility functions for adobe masonry buildings in the peruvian andes," *Frontiers in Built Environment*, 2020.
- [10] N. Giordano, F. De Luca, and A. Sextos, "Analytical fragility curves for masonry school building

- portfolios in Nepal,” *Bulletin of Earthquake Engineering*, 2021.
- [11] H. B. Ceran and M. A. Erberik, “Effect of out-of-plane behavior on seismic fragility of masonry buildings in Turkey,” *Bulletin of Earthquake Engineering*, 2013.
- [12] A. G. Simões, R. Bento, S. Lagomarsino, S. Cattari, and P. B. Lourenço, “Seismic assessment of nineteenth and twentieth centuries URM buildings in Lisbon: structural features and derivation of fragility curves,” *Bulletin of Earthquake Engineering*, 2020.
- [13] M. A. Jaimes, M. M. Chávez, F. Peña, and A. D. García-Soto, “Out-of-plane mechanism in the seismic risk of masonry façades,” *Bulletin of Earthquake Engineering*, 2021.
- [14] A. A. Costa, “Seismic assessment of the out-of-plane performance of traditional stone masonry walls (PhD Thesis). Faculty of Engineering, University of Porto,” FEUP, Porto, 2012.
- [15] T. M. Ferreira, A. A. Costa, R. Vicente, and H. Varum, “A simplified four-branch model for the analytical study of the out-of-plane performance of regular stone URM walls,” *Engineering Structures*, 2015.
- [16] S. Lagomarsino and S. Cattari, “Fragility Functions of Masonry Buildings,” *Geotechnical, Geological and Earthquake Engineering*, 2014.
- [17] M. Rota, A. Penna, and G. Magenes, “A methodology for deriving analytical fragility curves for masonry buildings based on stochastic nonlinear analyses,” *Engineering Structures*, 2010.
- [18] J. Milosevic, S. Cattari, and R. Bento, “Definition of fragility curves through nonlinear static analyses: procedure and application to a mixed masonry-RC building stock,” *Bulletin of Earthquake Engineering*, 2020.
- [19] S. Lagomarsino, S. Cattari, and D. Ottonelli, “The heuristic vulnerability model: fragility curves for masonry buildings,” *Bulletin of Earthquake Engineering*, 2021.
- [20] V. Bernardo, R. Sousa, P. Candeias, A. Costa, and A. Campos Costa, “Historic Appraisal Review and Geometric Characterization of Old Masonry Buildings in Lisbon for Seismic Risk Assessment,” *International Journal of Architectural Heritage*, 2021.
- [21] P. Candeias *et al.*, “General aspects of the application in Portugal of Eurocode 8 – Part 3 – Annex C (Informative) – Masonry Buildings [in Portuguese],” *Revista Portuguesa de Engenharia de Estruturas*. RPEE série III, n° 12, Lisbon, Portugal [in Portuguese], 2020.
- [22] M. J. Fryer and R. Y. Rubinstein, “Simulation and the Monte Carlo Method.,” *Journal of the Royal Statistical Society. Series A (General)*, 1983.
- [23] S. Lagomarsino, A. Penna, A. Galasco, and S. Cattari, “TREMURI program: An equivalent frame model for the nonlinear seismic analysis of masonry buildings,” *Engineering Structures*, 2013.
- [24] V. Bernardo, A. Campos Costa, P. Candeias, and A. Costa, “Seismic Vulnerability Assessment and Fragility Analysis of Pre-code Masonry Buildings in Portugal (under review - BEEE-D-21-00264R2),” *Bulletin of Earthquake Engineering*, 2021.
- [25] A. G. Simões, R. Bento, S. Lagomarsino, S. Cattari, and P. B. Lourenço, “The seismic assessment of masonry buildings between the 19th and 20th centuries in Lisbon-evaluation of uncertainties,” in *Proceedings of the International Masonry Society Conferences*, 2018.
- [26] CEN, *Eurocode 8: Design of structures for earthquake resistance - Part 1: General rules, seismic actions and rules for buildings*. Brussels, Belgium: Comité Européen de Normalisation, 2004.
- [27] A. G. G. Simões, “Evaluation of the seismic vulnerability of the unreinforced masonry buildings constructed in the transition between the 19th and 20th centuries in Lisbon (PhD Thesis). Technical University of Lisbon, Lisbon, Portugal [in Portuguese], 2019.” 2018.
- [28] J. Milosevic, “Seismic vulnerability assessment of mixed masonry-reinforced concrete buildings in Lisbon (PhD Thesis),” Technical University of Lisbon, Lisbon, Portugal [in Portuguese], 2019.
- [29] A. Galasco, S. Lagomarsino, and A. Penna, “On the use of pushover analysis for existing masonry buildings,” *First European Conference on Earthquake Engineering and Seismology*, no. September, pp. 3–8, 2006.
- [30] S. Lagomarsino and S. Cattari, “Seismic performance of historical masonry structures through pushover and nonlinear dynamic analyses,” *Geotechnical, Geological and Earthquake Engineering*, 2015.